Title

Carboxyl-terminal sequences in APOA5 are important for suppressing ANGPTL3/8 activity.

Journal

Proceedings of the National Academy of Sciences, 121(17)

Authors

Chen, Yan
Yang, Ye
Zhen, Eugene
et al.

Publication Date

2024-04-23

DOI

10.1073/pnas.2322332121

Peer reviewed

PNAS RESEARCH ARTICLE | MEDICAL SCIENCES

Carboxyl-terminal sequences in APOA5 are important for suppressing ANGPTL3/8 activity

Yan Q. Chen[a,1], Ye Yang[b,c,1], Eugene Y. Zhen[a], Thomas P. Beyer[a], Hongxia Li[a], Yi Wen[a], Mariam Ehsani[a], Nicholas Jackson[b], Katherine Xie[b], Hyesoo Jung[b], Julia L. Scheithauer[b], Anni Kumari[d,e], Gabriel Birrane[f], Anna M. Russell[a], Deepa Balasubramaniam[a], Zhongping Liao[a], Robert W. Siegel[a], Yuewei Qian[a], Michael Ploug[d,e], Stephen G. Young[b,c,2], and Robert J. Konrad[a,2]

Contributed by Stephen G. Young; received December 24, 2023; accepted March 16, 2024; reviewed by Sander Kersten and Renate Schreiber

Apolipoprotein AV (APOA5) lowers plasma triglyceride (TG) levels by binding to the angiopoietin-like protein 3/8 complex (ANGPTL3/8) and suppressing its capacity to inhibit lipoprotein lipase (LPL) catalytic activity and its ability to detach LPL from binding sites within capillaries. However, the sequences in APOA5 that are required for suppressing ANGPTL3/8 activity have never been defined. A clue to the identity of those sequences was the presence of severe hypertriglyceridemia in two patients harboring an *APOA5* mutation that truncates APOA5 by 35 residues ("APOA5Δ35"). We found that wild-type (WT) human APOA5, but not APOA5Δ35, suppressed ANGPTL3/8's ability to inhibit LPL catalytic activity. To pursue that finding, we prepared a mutant mouse APOA5 protein lacking 40 C-terminal amino acids ("APOA5Δ40"). Mouse WT-APOA5, but not APOA5Δ40, suppressed ANGPTL3/8's capacity to inhibit LPL catalytic activity and sharply reduced plasma TG levels in mice. WT-APOA5, but not APOA5Δ40, increased intracapillary LPL levels and reduced plasma TG levels in *Apoa5*$^{-/-}$ mice (where TG levels are high and intravascular LPL levels are low). Also, WT-APOA5, but not APOA5Δ40, blocked the ability of ANGPTL3/8 to detach LPL from cultured cells. Finally, an antibody against a synthetic peptide corresponding to the last 26 amino acids of mouse APOA5 reduced intracapillary LPL levels and increased plasma TG levels in WT mice. We conclude that C-terminal sequences in APOA5 are crucial for suppressing ANGPTL3/8 activity in vitro and for regulating intracapillary LPL levels and plasma TG levels in vivo.

ANGPTL3/8 | apolipoprotein AV | triglycerides | lipoprotein lipase

Significance

Apolipoprotein AV (APOA5) binds to the angiopoietin-like protein 3/8 complex (ANGPTL3/8) and suppresses its ability to inhibit lipoprotein lipase (LPL), but the APOA5 sequences required for regulating ANGPTL3/8 have never been defined. We found that wild-type (WT) human APOA5, but not truncated APOA5 proteins associated with hypertriglyceridemia, blocked the capacity of ANGPTL3/8 to inhibit LPL activity. Mouse WT-APOA5, but not a truncated APOA5 lacking 40 C-terminal amino acids, increased intracapillary LPL levels in *Apoa5*$^{-/-}$ mice and sharply reduced plasma triglyceride levels. Also, WT-APOA5, but not the truncated APOA5, blocked ANGPTL3/8-mediated detachment of LPL from cultured cells. Thus, carboxyl-terminal sequences in APOA5 are crucial for suppressing ANGPTL3/8 activity. Our findings explain the hypertriglyceridemia in patients with truncating *APOA5* mutations.

For more than 20 y, apolipoprotein AV (APOA5) has been recognized as a regulator of plasma triglyceride (TG) metabolism, evident from hypertriglyceridemia in *Apoa5*$^{-/-}$ mice and the fact that overexpression of human APOA5 reduces plasma TG levels (1). APOA5 is a PPARα-responsive apolipoprotein produced by the liver (2–4). APOA5 is found on chylomicrons, VLDL, and HDL, but APOA5 concentrations in the plasma (~6 nM) are much lower than levels of other apolipoproteins (which are present in μM levels) (5–7). The APOA5 sequences that form lipid-binding amphipathic α-helices (8, 9) and a heparin-binding domain (10) have been defined, but for many years the mechanism by which APOA5 regulates plasma TG metabolism has remained a mystery. Over the past 2 y, however, the mechanism for APOA5 function has come into focus. Chen et al. (11) found that APOA5 binds to the angiopoietin-like protein 3/8 complex (ANGPTL3/8) and suppresses its ability to inhibit the catalytic activity of lipoprotein lipase (LPL). This observation suggested that ANGPTL3/8 activity would be higher (i.e., unsuppressed) in the absence of APOA5, leading to increased inhibition of LPL activity and higher plasma TG levels. Consistent with that model, an inhibitory ANGPTL3/8-specific monoclonal antibody (mAb) reduces plasma TG levels in both mice and humans with hyperlipidemia (12, 13).

Recent studies by Yang et al. (14) added to our understanding of APOA5 and ANGPTL3/8 physiology; they found that amounts of LPL on the luminal surface of capillaries in heart and brown adipose tissue (BAT) are lower in *Apoa5*$^{-/-}$ mice than in *Apoa5*$^{+/+}$ mice. That finding led them to predict that APOA5 not only suppresses the ability of ANGPTL3/8 to inhibit LPL activity but also prevents ANGPTL3/8 from detaching LPL from its binding sites within capillaries. In support of that idea, they found that recombinant ANGPTL3/8 detached LPL from the surface of cultured cells and that ANGPTL3/8-mediated detachment of LPL could be blocked by recombinant APOA5 and by an inhibitory ANGPTL3/8-specific mAb (14). Both recombinant APOA5 and the inhibitory ANGPTL3/8 mAb increased intracapillary LPL levels in *Apoa5*$^{-/-}$ mice, resulting in sharply reduced plasma TG levels (14).

Reviewers: S.K., Wageningen University & Research; and R.S., Karl-Franzens-Universitat Graz.

Competing interest statement: S.G.Y. is on the scientific advisory board of Kyttaro; he has received consulting fees from Kyttaro and holds stock in that company. All authors from Eli Lilly & Co. own stock in the company.

[1]Y.Q.C. and Y.Y. contributed equally to this work.

[2]To whom correspondence may be addressed. Email: sgyoung@mednet.ucla.edu or konrad_robert@lilly.com.

This article contains supporting information online at https://www.pnas.org/lookup/suppl/doi:10.1073/pnas.2322332121/-/DCSupplemental.

Published April 16, 2024.

Despite progress in understanding APOA5's function, the APOA5 sequences that are important for suppressing ANGPTL3/8 activity have remained a mystery. In considering this issue, we were intrigued by the observation that a pair of *APOA5* mutations (Q275X and D332VfsX4, which truncate APOA5 by 92 and 35 residues, respectively) are associated with severe hypertriglyceridemia (chylomicronemia) (15, 16). A 70-y-old compound heterozygote (Q275X and Q97X mutations) had plasma TG levels >8,000 mg/dL; a 4-y-old compound heterozygote (Q97X and D332VfsX4 mutations) had TG levels >1,500 mg/dL; and a 35-y-old D332VfsX4 homozygote had TG levels >2,500 mg/dL (15, 16). Based on those observations, we wanted to test whether truncated APOA5 proteins retain the ability to suppress ANGPTL3/8 activity.

We recognized that performing assays of LPL catalytic activity would be insufficient to understand the effects of APOA5 truncations. It was clear to us that we would need to define the impact of APOA5 truncations on plasma TG levels and intracapillary LPL levels in hypertriglyceridemic mice (including *Apoa5*$^{-/-}$ mice). We recognized that mouse experiments would require us to examine the effects of recombinant *mouse* proteins. Accordingly, we produced mouse WT-APOA5 and a mutant mouse APOA5 lacking 40 C-terminal residues ("APOA5Δ40") and examined their effects on ANGPTL3/8-mediated inhibition of LPL catalytic activity, ANGPTL3/8-mediated detachment of LPL from cultured cells, and plasma TG levels and intracapillary LPL levels in *Apoa5*$^{-/-}$ mice.

Results

Truncated Human APOA5 Proteins Do Not Suppress the Ability of the ANGPTL3/8 Complex to Inhibit LPL Activity. We were intrigued by reports of chylomicronemia in patients with truncating *APOA5* mutations (15, 16). To determine whether truncated APOA5 proteins are functionally defective, we expressed and purified human WT-APOA5 and the truncated APOA5 proteins resulting from the Q275X and D332VfsX4 mutations. The Q275X mutation eliminates 92 C-terminal residues ("APOA5Δ92"); the D332VfsX4 mutation eliminates 35 residues ("APOA5Δ35"). We compared the ability of human WT-APOA5 and the truncated APOA5 proteins to suppress the capacity of human ANGPTL3/8 to inhibit the catalytic activity of human LPL. WT-APOA5 blocked ANGPTL3/8-mediated inhibition of LPL activity, whereas recombinant APOA5Δ92 and APOA5Δ35 did not (Fig. 1). We also showed that an ANGPTL3/8-specific mAb (IBA490) blocked the ability of ANGPTL3/8 to inhibit LPL activity (Fig. 1).

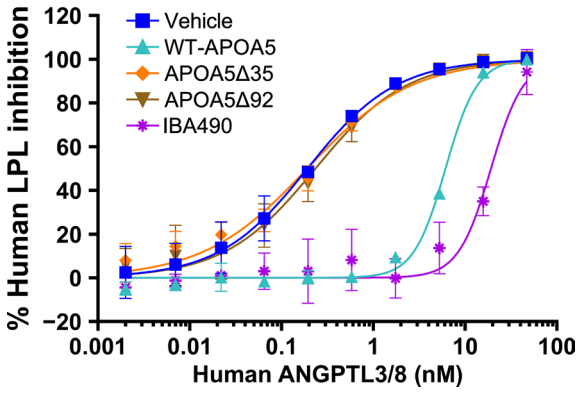

Fig. 1. Human WT-APOA5, but not human APOA5Δ35 or human APOA5Δ92, suppresses human ANGPTL3/8-mediated inhibition of LPL catalytic activity. HEK293 cells expressing human LPL were incubated in medium containing increasing concentrations of human ANGPTL3/8 that had been preincubated with 20 nM human WT-APOA5, APOA5Δ35, APOA5Δ92, the inhibitory ANGPTL3/8 mAb IBA490, or vehicle (PBS) alone; IC_{50} values for inhibition of LPL catalytic activity by ANGPTL3/8 were 6.14, 0.19, 0.23, 19.20, and 0.19 nM, respectively. Results show mean ± SD (*n* = 3 to 5 from three independent experiments).

Recombinant Proteins. We prepared recombinant proteins (human ANGPTL3/8, mouse ANGPTL3/8, human APOA5, and mouse APOA5) and then examined the ability of the different APOA5 proteins to suppress ANGPTL3/8-mediated inhibition of LPL catalytic activity. Mouse ANGPTL3/8 inhibited human LPL with an IC_{50} of 0.46 nM, whereas human ANGPTL3/8 inhibited human LPL with an IC_{50} of

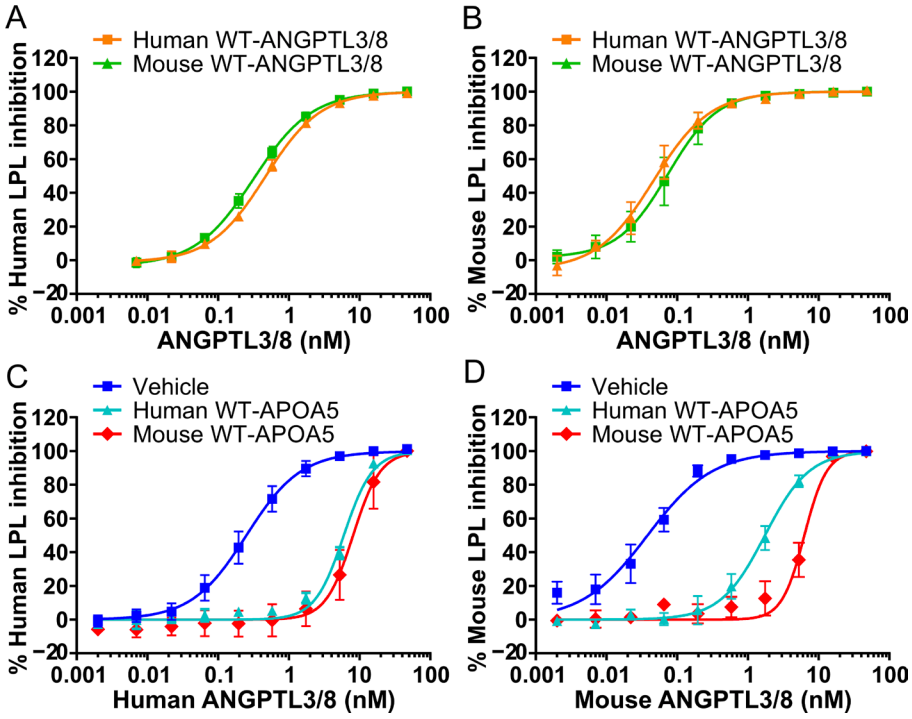

Fig. 2. Characterizing recombinant mouse proteins. (*A*) Human and mouse ANGPTL3/8 inhibit human LPL with IC_{50} values of 0.32 nM and 0.46 nM, respectively. Results show mean ± SD; *n* = 4 measurements; two independent experiments. (*B*) Mouse LPL is 4.4-fold more susceptible than human LPL to inhibition by human ANGPTL3/8 and 9.3-fold more susceptible to inhibition by mouse ANGPTL3/8 (IC_{50} values of 0.073 nM and 0.050 nM, respectively). Results show mean ± SD; *n* = 6 measurements; three independent experiments. (*C*) Human WT-APOA5 and mouse WT-APOA5 suppress human ANGPTL3/8-mediated inhibition of LPL activity (IC_{50} values of 6.00 nM and 8.12 nM, respectively). Results show mean ± SD; *n* = 3 to 5 measurements; three independent experiments. (*D*) Mouse WT-APOA5 is 3.6-fold more potent than human WT-APOA5 in suppressing mouse ANGPTL3/8-mediated inhibition of mouse LPL activity (IC_{50} values of 6.28 nM and 1.74 nM, respectively). Results show mean ± SD; *n* = 5 measurements; three independent experiments.

0.32 nM (Fig. 2*A*). Mouse LPL was 4.4-fold more susceptible than human LPL to inhibition by human ANGPTL3/8 and 9.3-fold more susceptible to inhibition by mouse ANGPTL3/8 (Fig. 2*B*). Mouse WT-APOA5 and human WT-APOA5 had comparable abilities to suppress human ANGPTL3/8 activity (Fig. 2*C*), but mouse WT-APOA5 was 3.6-fold more potent than human WT-APOA5 in suppressing mouse ANGPTL3/8 activity (Fig. 2*D*).

Serum Levels of TGs, ANGPTL3/8, and APOA5 in WT Mice. We measured serum levels of triglycerides (TGs), ANGPTL3/8, and APOA5 in WT mice during fasting and 4 h after refeeding. TG levels were higher after feeding (89.4 ± 25.7 mg/dL vs. 67.4 ± 12.3 mg/dL during fasting) (Table 1). ANGPTL3/8 levels increased after feeding (565.2 ± 166.2 pM vs. 63.6 ± 23.4 pM during fasting) (Table 1). Mouse APOA5 levels were lower after feeding (4.4 ± 1.0 nM vs. 5.8 ± 0.9 nM during fasting) (Table 1).

A Truncated Mouse APOA5 Does Not Bind to ANGPTL3/8 or Suppress ANGPTL3/8 Activity. To assess the properties of a truncated version of mouse APOA5, we expressed and purified mouse WT-APOA5 and a truncated mouse APOA5 lacking 40 C-terminal residues ("APOA5Δ40"). [APOA5Δ40 results from the same mutation that causes APOA5Δ35 in humans; mouse APOA5 has a five-residue C-terminal extension (explaining why the total number of deleted residues is greater in the mouse)]. The purity of mouse APOA5Δ40 was comparable to that of mouse WT-APOA5, as judged by Coomassie Blue staining (of reduced and nonreduced proteins), size-exclusion chromatography (SEC), and mass photometry (*SI Appendix*, Fig. S1 *A–E*). SEC revealed that mouse WT-APOA5 and APOA5Δ40 were mixtures of monomers and dimers (*SI Appendix*, Fig. S1 *B* and *C*); that finding was confirmed by mass photometry (*SI Appendix*, Fig. S1 *D* and *E*). Mouse APOA5Δ40 was not detected by western blotting with a rabbit polyclonal antibody (CT-APOA5 pAb) against the last 26 residues in mouse APOA5, nor was it detected by a sandwich immunoassay that used an N-terminal APOA5 mAb (NT-APOA5 mAb) for capture and the CT-APOA5 pAb for detection (*SI Appendix*, Fig. S2 *A* and *B*). Surface plasmon resonance (SPR) studies revealed that APOA5Δ40 cannot bind to ANGPTL3/8, whereas mouse WT-APOA5 binds to ANGPTL3/8 with a nanomolar affinity (K_d = 0.53 nM) (Fig. 3*A*). Consistent with that finding, mouse WT-APOA5 (but not APOA5Δ40) blocked the capacity of mouse ANGPTL3/8 to inhibit the catalytic activity of mouse LPL (Fig. 3*B*). In these studies, the ability of mouse ANGPTL3/8 to inhibit LPL was blocked by IBA490, and we confirmed that human WT-APOA5 (but not human APOA5Δ35) inhibited ANGPTL3/8 activity (Fig. 3*B*).

Mouse WT-APOA5, but Not APOA5Δ40, Reduces TG Levels in CETP/APOA1 Transgenic Mice and *Apoa5*$^{-/-}$ Mice. To assess the activity of the mouse APOA5 proteins in vivo, CETP/APOA1 transgenic mice [which have baseline serum TG levels of ~500 mg/dL (12)] were given an injection of mouse WT-APOA5, mouse APOA5Δ40, mAb IBA490, or vehicle (PBS) alone. Serum TG levels were measured at baseline and 1, 3, and 6 h later (Fig. 4*A*). Mouse WT-APOA5 and mAb IBA490 sharply reduced serum TG levels, whereas APOA5Δ40 did not (Fig. 4*A*). We observed similar findings in *Apoa5*$^{-/-}$ mice; mouse WT-APOA5 and IBA490 sharply reduced plasma TG levels, whereas APOA5Δ40 did not (Fig. 4*B*).

Table 1. Serum TG, ANGPTL3/8, and APOA5 levels in C57BL/6 mice after an overnight fast and after refeeding with a chow diet for 4 h

	TG (mg/dL)	ANGPTL3/8 (pM)	APOA5 (nM)
Fasted (*n* = 10)	67.4 ± 12.3	63.6 ± 23.4	5.8 ± 0.9
Refed (*n* = 10)	89.4 ± 25.7	565.2 ± 166.2	4.4 ± 1.0
P	0.025	<0.0001	0.0045

Results show mean ± SD; differences were analyzed with an unpaired Student's *t* test.

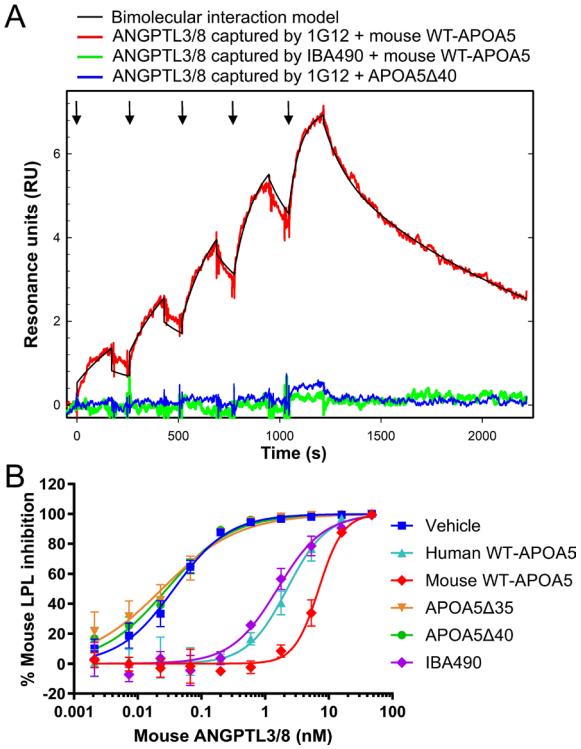

Fig. 3. Mouse WT-APOA5, but not mouse APOA5Δ40, binds ANGPTL3/8 and suppresses ANGPTL3/8-mediated inhibition of LPL activity. (*A*) Real-time SPR binding of APOA5 to ANGPTL3/8. A rabbit anti-mouse IgG coupled to CM4 sensor chip was primed with ANGPTL3/8-specific mAb 1G12 (which recognizes ANGPTL3's C-terminal fibrinogen-like domain) or mAb IBA490 (which recognizes the APOA5-binding region in ANGPTL3/8). After an injection of 25 nM ANGPTL3/8, comparable levels of ANGPTL3/8 were captured by 1G12 and IBA490. For the ligand binding event, serial twofold dilutions of 0.5 to 8 nM mouse WT-APOA5 or mouse APOA5Δ40 were injected (arrows). WT-APOA5 bound with high affinity to ANGPTL3/8 captured on 1G12 (red curve) but did not bind to the ANGPTL3/8 captured on IBA490 (green curve). The binding of APOA5 to 1G12 captured–ANGPTL3/8 fit to a simple bimolecular interaction model (thin black line) and yielded an association rate (k_{on}) of 1.57 ± 0.04 × 10^6 $M^{-1}s^{-1}$ and a dissociation rate (k_{off}) of 8.32 ± 0.02 × 10^{-4} s^{-1}, resulting in a dissociation constant (K_d) of 0.53 nM. There was no binding of APOA5Δ40 when it was injected over 1G12 captured–ANGPTL3/8 (blue curve). (*B*) Assessing the ability of APOA5 proteins to suppress ANGPTL3/8–mediated inhibition of LPL catalytic activity. Mouse LPL–expressing cells were incubated with medium containing increasing concentrations of mouse ANGPTL3/8 that had been preincubated with 20 nM APOA5 proteins (human WT-APOA5, mouse WT-APOA5, human APOA5Δ35, mouse APOA5Δ40), 20 nM IBA490, or vehicle alone; IC_{50} values for LPL activity inhibition by ANGPTL3/8 were 2.18, 6.90, 0.023, 0.028, 1.54, and 0.036 nM, respectively. Results show mean ± SD (*n* = 3 independent experiments).

Recombinant Mouse WT-APOA5, but Not APOA5Δ40, Increases Intracapillary LPL Levels in *Apoa5*$^{-/-}$ Mice. We suspected that the lower plasma TG levels in *Apoa5*$^{-/-}$ mice after an injection of WT-APOA5 resulted from increased amounts of LPL in capillaries. To test that suspicion, *Apoa5*$^{-/-}$ mice were given an intravenous injection of WT-APOA5, APOA5Δ40, or PBS alone (n = 6 mice/group),

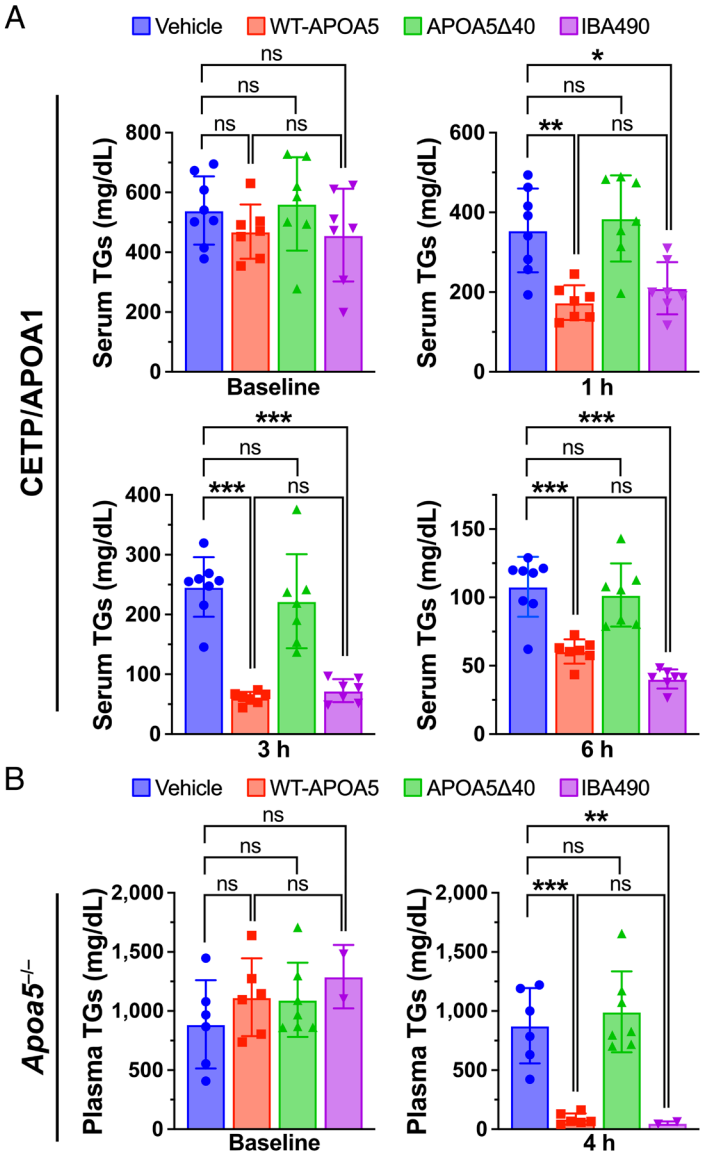

Fig. 4. Mouse WT-APOA5, but not mouse APOA5Δ40, lowers TG levels in CETP/APOA1 and *Apoa5*$^{-/-}$ mice. (*A*) Serum TG levels in CETP/APOA1 transgenic mice (n = 7 to 8/group) after a single dose of mouse WT-APOA5 (1 nmole), APOA5Δ40 (1 nmole), IBA490 (2.5 nmole), or vehicle (PBS). TG levels were measured at baseline and 1 h, 3 h, and 6 h after the injection. (*B*) Plasma TG levels in *Apoa5*$^{-/-}$ mice (n = 6 to 7/group) after a single intravenous injection of mouse WT-APOA5 (0.5 nmole), mouse APOA5Δ40 (0.5 nmole), or vehicle (PBS) alone. As a control, IBA490 (1.25 nmole) was given to *Apoa5*$^{-/-}$ mice (n = 2/group). TG levels were measured at baseline and 4 h after the injection. Data show mean ± SD in (*A*) and (*B*). A one-way ANOVA test revealed that wild-type and truncated APOA5 proteins had distinct effects on TG levels in CETP/APOA1 and *Apoa5*$^{-/-}$ mice. Tukey's HSD ("honestly significant difference") post hoc test revealed that mouse WT-APOA5, but not APOA5Δ40, significantly reduced TG levels. *P < 0.05; **P < 0.025; ***P < 0.001; ns, not significant.

followed 4 h later by an intravenous injection of IRDye-labeled mAbs 27A7 (against mouse LPL) and 11A12 (against the endothelial cell protein GPIHBP1). Sections of the entire heart and an entire BAT pad were prepared, and both IRDye signals were quantified with an infrared scanner. This method for quantifying intravascular LPL levels is useful because i) a large expanse of tissue is examined; ii) background infrared signals are negligible; iii) quantification of IRDyes with an infrared scanner has a linear range of >4,000-fold (17). The WT-APOA5 treatment significantly increased mAb 27A7 binding, relative to 11A12 binding, in the heart, reflecting increased amounts of LPL inside blood vessels (Fig. 5 *A*, *C*, and *E* and *SI Appendix*, Fig. S3). In contrast, the injection of APOA5Δ40 did not alter intravascular LPL levels (Fig. 5 *A*, *C*, and *E* and *SI Appendix*, Fig. S3). Similar findings were observed in BAT; WT-APOA5, but not APOA5Δ40, significantly increased amounts of LPL in blood vessels (Fig. 5 *B*, *D*, and *F* and *SI Appendix*, Fig. S3).

To visualize the changes in LPL levels in capillaries, we performed confocal immunofluorescence microscopy studies. *Apoa5*$^{-/-}$ mice were given an intravenous injection of mouse WT-APOA5, APOA5Δ40, or PBS. After 4 h, the mice were given an intravenous injection of Alexa Fluor–labeled 27A7, 11A12, and 2H8 (which is a mAb against the endothelial cell protein CD31). After 10 min, the vasculature was perfused with PBS and perfusion-fixed with 4% PFA. In four independent experiments, fluorescence microscopy of heart sections revealed that WT-APOA5, but not APOA5Δ40, increased amounts of LPL inside capillaries (relative to GPIHBP1 or CD31) (Fig. 6 *A*–*E* and *SI Appendix*, Fig. S4).

We performed two independent confocal microscopy studies of intracapillary LPL levels in BAT. Consistent with the IRDye experiments presented in Fig. 5, we found that WT-APOA5, but not APOA5Δ40, increased intracapillary LPL levels in BAT (*SI Appendix*, Fig. S5).

Mouse WT-APOA5, but Not APOA5Δ40, Blocks the Ability of ANGPTL3/8 to Detach LPL from Cultured Cells. Yang et al. (14) recently showed that the unsuppressed ANGPTL3/8 activity in *Apoa5*$^{-/-}$ mice not only inhibited LPL catalytic activity but also detached LPL from binding sites within capillaries. Also, studies by Song et al. (18) revealed that much of the LPL that is transported into capillaries detaches from GPIHBP1 and is captured within the heparan sulfate proteoglycan (HSPG)–rich endothelial cell

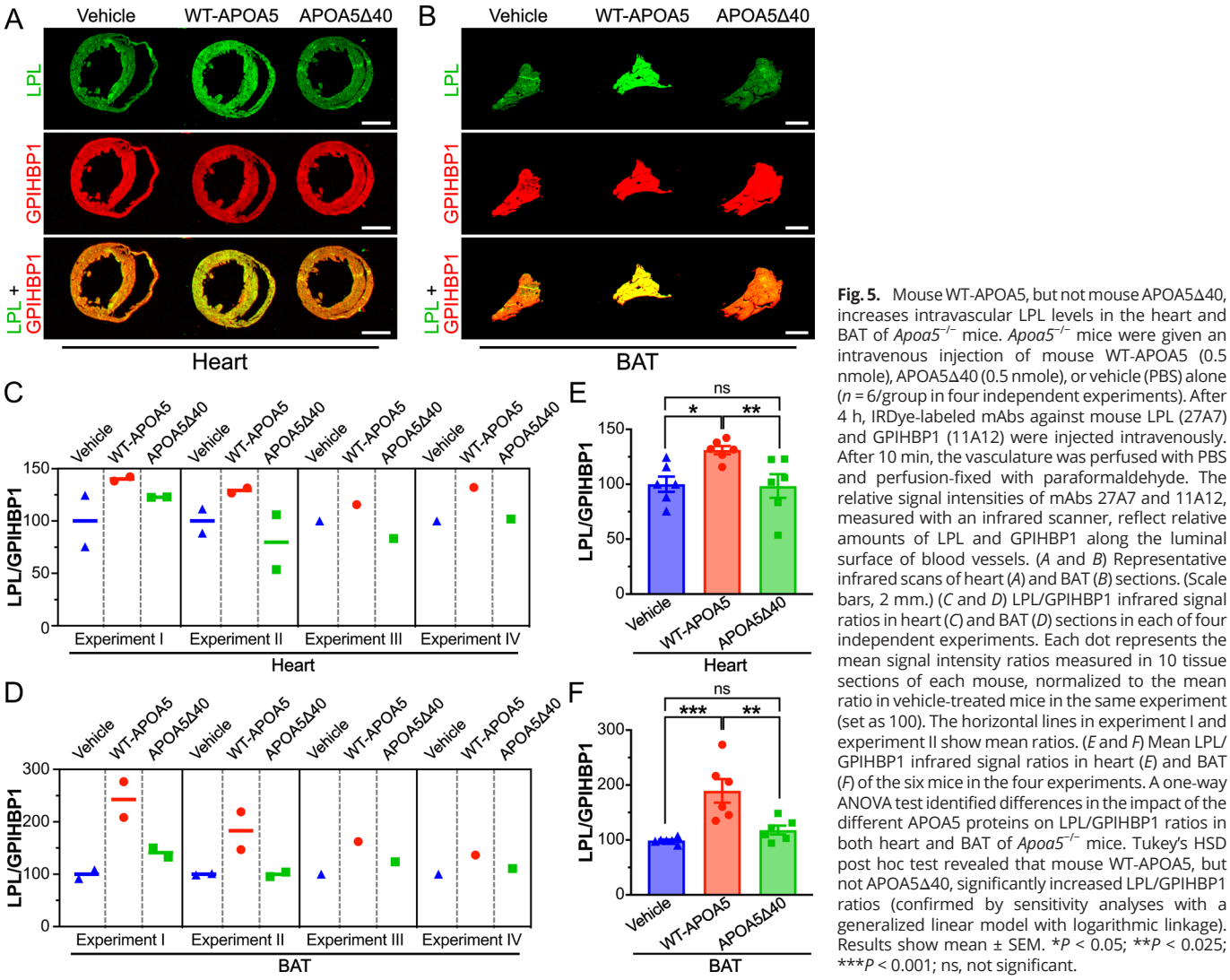

Fig. 5. Mouse WT-APOA5, but not mouse APOA5Δ40, increases intravascular LPL levels in the heart and BAT of *Apoa5*$^{-/-}$ mice. *Apoa5*$^{-/-}$ mice were given an intravenous injection of mouse WT-APOA5 (0.5 nmole), APOA5Δ40 (0.5 nmole), or vehicle (PBS) alone (n = 6/group in four independent experiments). After 4 h, IRDye-labeled mAbs against mouse LPL (27A7) and GPIHBP1 (11A12) were injected intravenously. After 10 min, the vasculature was perfused with PBS and perfusion-fixed with paraformaldehyde. The relative signal intensities of mAbs 27A7 and 11A12, measured with an infrared scanner, reflect relative amounts of LPL and GPIHBP1 along the luminal surface of blood vessels. (*A* and *B*) Representative infrared scans of heart (*A*) and BAT (*B*) sections. (Scale bars, 2 mm.) (*C* and *D*) LPL/GPIHBP1 infrared signal ratios in heart (*C*) and BAT (*D*) sections in each of four independent experiments. Each dot represents the mean signal intensity ratios measured in 10 tissue sections of each mouse, normalized to the mean ratio in vehicle-treated mice in the same experiment (set as 100). The horizontal lines in experiment I and experiment II show mean ratios. (*E* and *F*) Mean LPL/GPIHBP1 infrared signal ratios in heart (*E*) and BAT (*F*) of the six mice in the four experiments. A one-way ANOVA test identified differences in the impact of the different APOA5 proteins on LPL/GPIHBP1 ratios in both heart and BAT of *Apoa5*$^{-/-}$ mice. Tukey's HSD post hoc test revealed that mouse WT-APOA5, but not APOA5Δ40, significantly increased LPL/GPIHBP1 ratios (confirmed by sensitivity analyses with a generalized linear model with logarithmic linkage). Results show mean ± SEM. *P < 0.05; **P < 0.025; ***P < 0.001; ns, not significant.

glycocalyx. To explore the idea that mouse WT-APOA5 and APOA5Δ40 differ in their capacities to suppress ANGPTL3/8-mediated detachment of LPL, we prepared CHO-K1 cells and loaded the cell-surface HSPGs with recombinant human LPL. After washing, the cells were incubated for 15 min at 37 °C with mouse ANGPTL3/8 alone or ANGPTL3/8 in the presence of either mouse WT-APOA5 or APOA5Δ40. Nonpermeabilized cells were then stained with an Alexa Fluor 555–conjugated LPL-specific mAb (5D2); amounts of LPL on the surface of cells (as judged by 5D2 staining) were assessed by fluorescence microscopy. In three independent experiments, we found that ANGPTL3/8 detached LPL from cells and that the ANGPTL3/8-mediated LPL detachment was blocked by WT-APOA5 but not APOA5Δ40 (Fig. 7 *A* and *B* and *SI Appendix*, Fig. S6 *A* and *B*).

An Antibody against C-terminal Sequences in Mouse APOA5 Neutralizes the Impact of APOA5 on ANGPTL3/8 Activity In Vitro and Increases Plasma TG Levels In Vivo. Our studies with human APOA5Δ35 and mouse APOA5Δ40 implied that C-terminal sequences in APOA5 are important for suppressing ANGPTL3/8 activity. To explore that possibility, we developed a rabbit polyclonal antibody against the C-terminal 26 residues of mouse APOA5 (CT-APOA5 pAb) and tested the ability of that antibody to inhibit the ability of WT-APOA5 to suppress ANGPTL3/8 activity. As a control, we tested a mixture of mAbs against the N-terminal 23 residues of mouse APOA5 (NT-APOA5 mAbs). CT-APOA5 pAb bound to WT-APOA5 but not APOA5Δ40, whereas the NT-APOA5 mAbs bound to both WT-APOA5 and APOA5Δ40 (*SI Appendix*, Fig. S2 *A–C*). The ability of WT-APOA5 to suppress ANGPTL3/8-mediated inhibition of LPL activity was blocked by CT-APOA5 pAb but not by NT-APOA5 mAbs (Fig. 8*A*).

The finding that CT-APOA5 pAb neutralized the impact of WT-APOA5 to suppress ANGPTL3/8's ability to inhibit LPL catalytic activity prompted us to examine the effects of CT-APOA5 pAb on plasma TG levels in WT mice (FVB/NJ strain). The mice were fasted for 18 h and then given an intravenous injection of CT-APOA5 pAb or an injection of rabbit IgG purified from nonimmune rabbit serum (control IgG). The mice were then refed a chow diet. Plasma TG levels were measured at baseline (T0, immediately after the antibody infusion) and after 6 h of refeeding (T6). TG levels in the CT-APOA5 pAb–treated mice increased from 96.2 ± 22.5 mg/dL at T0 to 304.7 ± 74.5 mg/dL at T6 (P < 0.0001); no significant changes in TG levels were observed in mice treated with the control IgG (Fig. 8*B*). Neither CT-APOA5 pAb nor the control IgG changed TG levels in *Apoa5*$^{-/-}$ mice (Fig. 8*C*).

LPL levels in capillaries of mice that had received CT-APOA5 pAb were assessed with an intravenous injection of Alexa Fluor–labeled mAbs 27A7, 11A12, and 2H8. Fluorescence microscopy revealed that

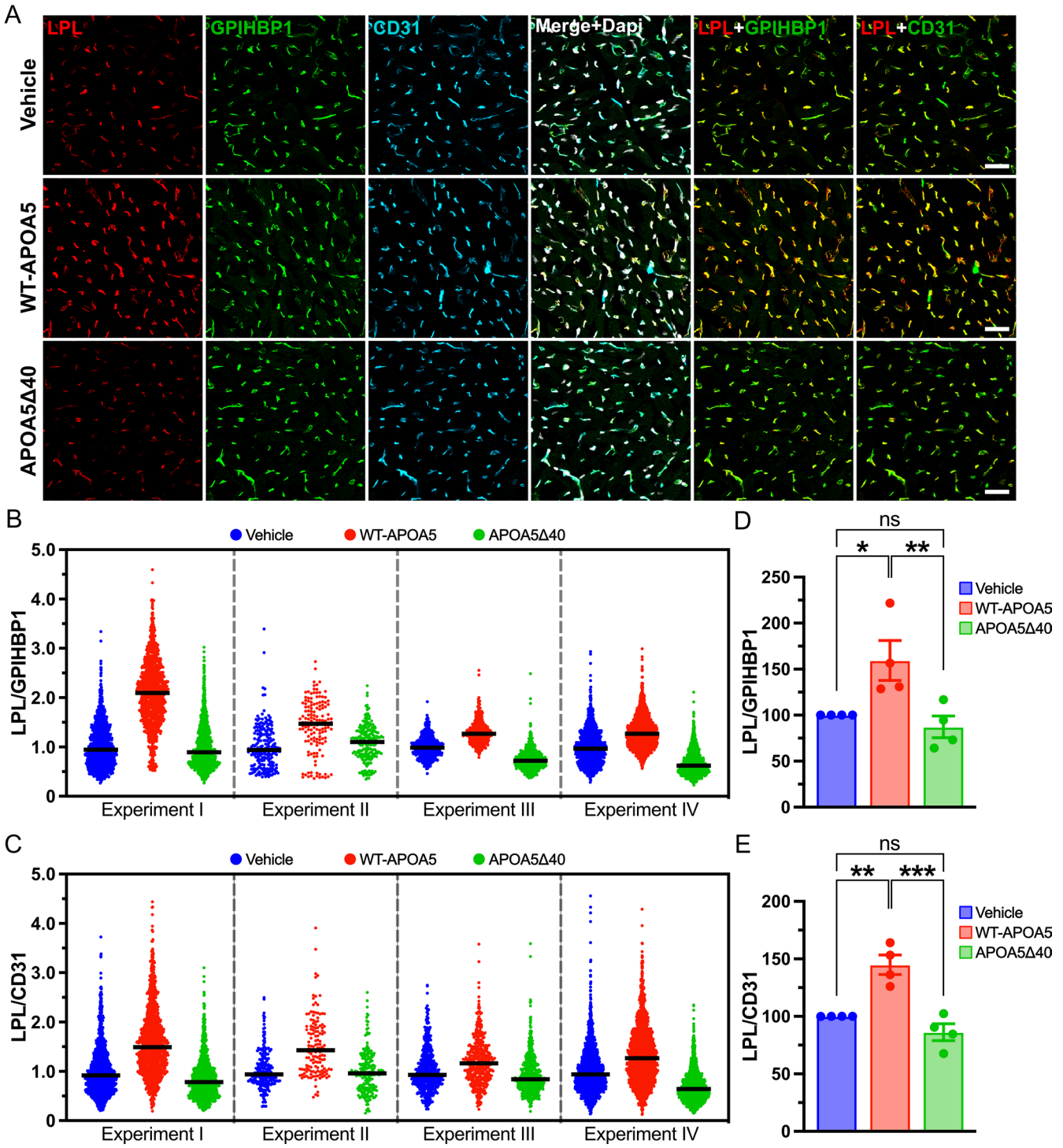

Fig. 6. Mouse WT-APOA5, but not mouse APOA5Δ40, increases intracapillary LPL levels in the heart of *Apoa5*$^{-/-}$ mice. *Apoa5*$^{-/-}$ mice were given an intravenous injection of mouse WT-APOA5 (0.5 nmole), mouse APOA5Δ40 (0.5 nmole), or vehicle (PBS) alone (one mouse per group in four independent experiments). After 4 h, the mice were given an intravenous injection of Alexa Fluor–labeled mAbs against mouse LPL (27A7), GPIHBP1 (11A12), and CD31 (2H8). After 10 min, the vasculature was perfused and fixed; tissue sections were prepared; and amounts of LPL, GPIHBP1, and CD31 along the luminal surface of heart capillaries were assessed by fluorescence microscopy. (*A*) Representative micrographs showing amounts of LPL, GPIHBP1, and CD31 in the heart of *Apoa5*$^{-/-}$ mice in experiment I. (Scale bars, 20 μm.) See *SI Appendix*, Fig. S3 for representative micrographs in experiments II, III, and IV. (*B* and *C*) LPL/GPIHBP1 (*B*) and LPL/CD31 (*C*) fluorescence intensity ratios in heart capillary segments. Each dot represents the ratio in one capillary segment (n = 146 to 1,774/heart); ratios were normalized to the mean fluorescence intensity ratios in heart capillaries of vehicle-treated mice (set as 1.0). The horizontal lines show the mean ratios in each mouse heart. (*D* and *E*) Mean LPL/GPIHBP1 (*D*) and LPL/CD31 ratios (*E*) in the heart in each of four independent experiments. Each dot represents the mean ratio in one mouse, normalized to the mean ratios in the heart of the vehicle-treated mice (set as 100). A one-way ANOVA found significant effect of APOA5 proteins on LPL/GPIHBP1 and LPL/CD31 ratios in the heart of *Apoa5*$^{-/-}$ mice. Tukey's HSD post hoc test showed that mouse WT-APOA5, but not APOA5Δ40, significantly increased LPL/GPIHBP1 and LPL/CD31 ratios (confirmed by sensitivity analyses with a generalized linear model with logarithmic linkage and SEs clustered by experiment). Results show mean ± SEM. *P < 0.05; **P < 0.025; ***P < 0.001; ns, not significant.

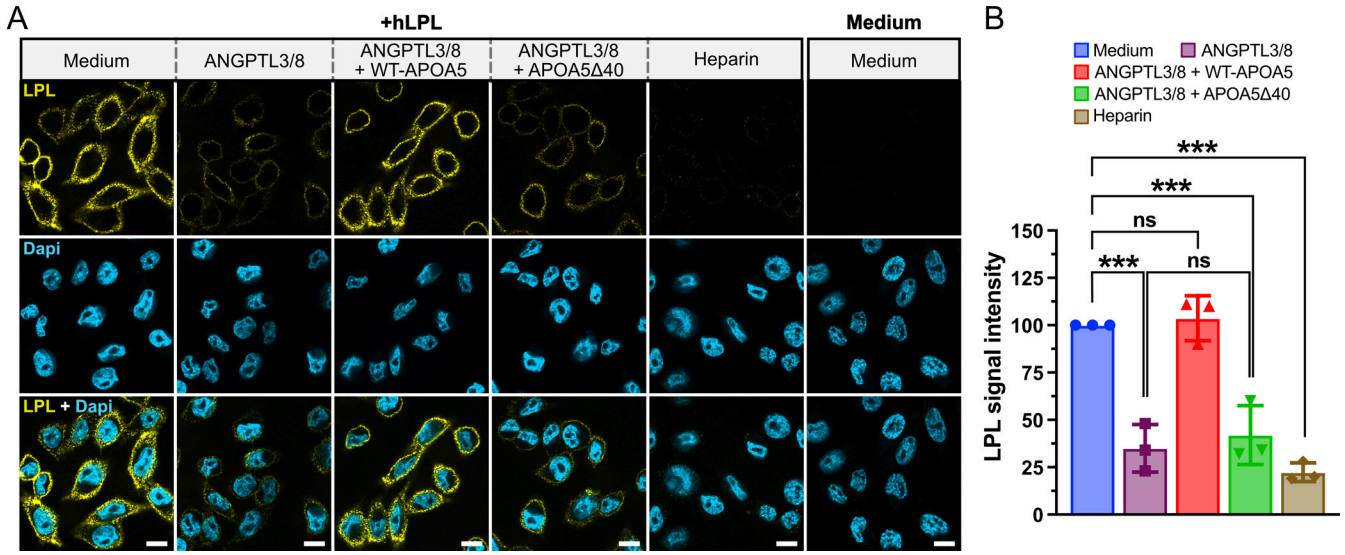

Fig. 7. Mouse WT-APOA5, but not mouse APOA5Δ40, inhibits ANGPTL3/8-mediated detachment of LPL from CHO-K1 cells. CHO-K1 cells were incubated in medium in the presence or absence of 50 nM human LPL (hLPL) at 37 °C for 10 min. After washing with PBS/Ca/Mg, the cells were incubated for 15 min at 37 °C with cell culture medium alone, 0.1 U/mL heparin, or 100 nM mouse ANGPTL3/8—either alone or in the presence of 1.4 μM mouse WT-APOA5 or 1.4 μM APOA5Δ40. (*A*) Amounts of hLPL on the surface of cells, as judged by fluorescence microscopy, after staining nonpermeabilized cells with Alexa Fluor 555–labeled mAb 5D2. (Scale bars, 10 μm.) (*B*) LPL remaining on the surface of CHO-K1 cells, as judged by mAb 5D2 fluorescence intensity, after treatment with heparin or treatment with ANGPTL3/8 (alone or in the presence of 1.4 μM mouse WT-APOA5 or 1.4 μM APOA5Δ40). Each dot represents the mean signal intensity in each treatment group, normalized to the mean intensity in culture medium–treated cells (set as 100). A one-way ANOVA found significant differences between mouse WT-APOA5 and APOA5Δ40 (in the presence of ANGPTL3/8) on amounts of LPL on the surface of cells. Tukey's HSD post hoc test found no significant differences in amounts of LPL on cells that had been incubated with medium alone and cells that had been incubated with ANGPTL3/8 + mouse WT-APOA5. Amounts of LPL on cells that had been incubated with heparin, ANGPTL3/8, or ANGPTL3/8 + APOA5Δ40 were significantly lower than in cells that had been incubated with medium alone. Similar results were found in sensitivity analyses from a generalized linear model with logarithmic linkage and SEs clustered by experiment. Results show mean ± SEM. ***$P < 0.001$; ns, not significant.

amounts of LPL in heart and BAT capillaries, relative to GPIHBP1 or CD31, were lower in mice that received CT-APOA5 pAb than in mice that received the control IgG (*SI Appendix*, Fig. S7 *A*–*C*). Given those findings, we predicted that CT-APOA5 pAb would interfere with the ability of WT-APOA5 to block ANGPTL3/8-mediated detachment of LPL from the surface of cultured cells. To test that prediction, CHO-K1 cells loaded with human LPL were incubated with medium alone, ANGPTL3/8 alone, ANGPTL3/8 with mouse WT-APOA5 or APOA5Δ40 that had been preincubated with CT-APOA5 pAb, or ANGPTL3/8 with mouse WT-APOA5 or APOA5Δ40 that had been preincubated with the control IgG. Amounts of LPL remaining on the surface of cells were assessed by staining the cells with Alexa Fluor 555–labeled 5D2 and then quantifying the fluorescent signal by confocal microscopy. Our prediction was upheld; in three independent experiments, CT-APOA5 (but not the control IgG) prevented WT-APOA5 from blocking ANGPTL3/8-mediated detachment of LPL from the surface of cells (Fig. 9 *A* and *B* and *SI Appendix*, Fig. S8 *A* and *B*).

Discussion

The observations that APOA5 suppresses the capacity of ANGPTL3/8 to inhibit LPL catalytic activity (11) and prevents ANGPTL3/8-mediated detachment of LPL from cultured cells (14) were important insights into the regulation of plasma TG metabolism (19). In the current study, we investigated the sequences within APOA5 required for APOA5's ability to regulate ANGPTL3/8 activity. We began by investigating human *APOA5* mutations, Q275X and D332VfsX4, that had been uncovered in patients with chylomicronemia (15, 16); those mutations truncate APOA5 by 92 and 35 residues, respectively. In biochemical assays, neither truncated APOA5 suppressed the ability of ANGPTL3/8 to inhibit LPL activity. That observation was consistent with the presence of chylomicronemia in affected patients, but we recognized that defining the impact of the truncations would necessitate experiments in mice. We went on to show that recombinant mouse WT-APOA5, but not a truncated mouse APOA5 (APOA5Δ40), suppressed the capacity of mouse ANGPTL3/8 to inactivate mouse LPL activity. We also found that mouse WT-APOA5 sharply reduced plasma TG levels in two lines of hypertriglyceridemic mice, whereas APOA5Δ40 did not. Consistent with those findings, an injection of WT-APOA5 (but not APOA5Δ40) increased amounts of LPL inside heart and BAT capillaries of *Apoa5*$^{-/-}$ mice. Also, WT-APOA5 (but not APOA5Δ40) blocked the capacity of ANGPTL3/8 to detach LPL from cultured cells. SPR made sense of all of these observations; WT-APOA5 bound to the ANGPTL3/8 complex with nM affinity, whereas there was no binding of APOA5Δ40.

The fact that WT-APOA5, but not APOA5Δ40, suppressed ANGPTL3/8 activity led us to predict that an antibody against C-terminal sequences in mouse APOA5 (CT-APOA5 pAb) would interfere the ability of APOA5 to suppress ANGPTL3/8 activity. Indeed, CT-APOA5 pAb interfered with the ability of WT-APOA5 to suppress ANGPTL3/8-mediated inhibition of LPL's TG hydrolase activity, and it prevented the capacity of WT-APOA5 to block ANGPTL3/8-mediated detachment of LPL from the cultured cells. Also, an injection of CT-APOA5 pAb into WT mice reduced intracapillary LPL levels and increased plasma TG levels.

We believe that the capacity of ANGPTL3/8 to inhibit LPL activity and detach LPL from cells are both manifestations of ANGPTL3/8's ability to unfold LPL. Hydrogen–deuterium exchange/mass spectrometry (HDX-MS) studies revealed that ANGPTL4 functions by unfolding LPL's hydrolase domain, resulting in collapse of the catalytic pocket and irreversible loss of catalytic activity (20–22). These observations were consistent with earlier studies showing that ANGPTL4 triggers intracellular degradation of LPL (23–25). We suspect that

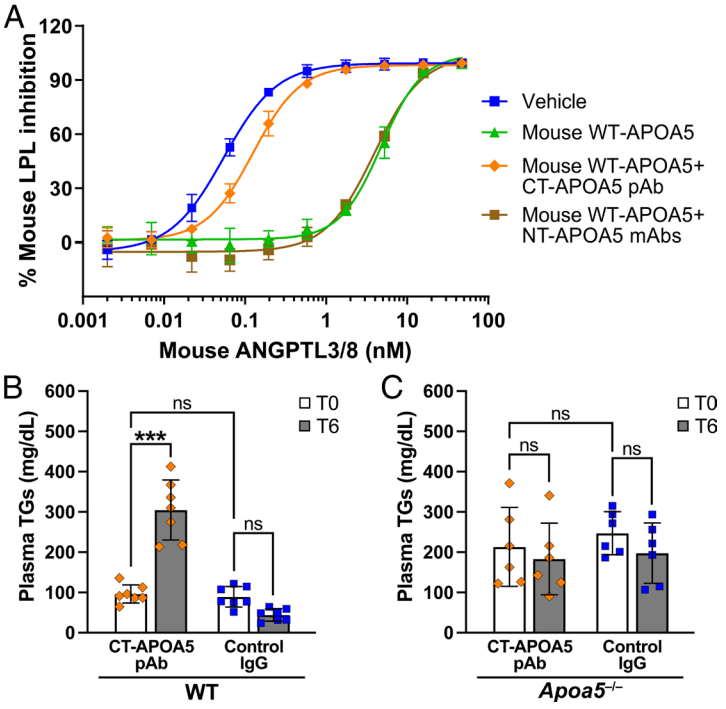

Fig. 8. An immunopurified rabbit polyclonal antibody against the C-terminal 26 residues of mouse WT-APOA5 (CT-APOA5 pAb) blocks the ability of APOA5 to suppress ANGPTL3/8-mediated inhibition of LPL activity in vitro and increases plasma TG levels in WT mice. (*A*) Mouse LPL–expressing cells were incubated with medium containing increasing concentrations of mouse ANGPTL3/8 that had been preincubated with vehicle alone, 20 nM mouse WT-APOA5, or 20 nM mouse WT-APOA5 in the presence of either CT-APOA5 pAb (1 μM) or NT-APOA5 mAbs (1 μM). Results show mean ± SD (n = 4 to 5 from three independent experiments). In the presence of NT-APOA5 mAbs, WT-APOA5 suppressed ANGPTL3/8-mediated inhibition of LPL activity (IC_{50}, 3.929 nM). CT-APOA5 pAb blocked WT-APOA5–mediated suppression of ANGPTL3/8 activity (IC_{50}, 0.126 nM). (*B* and *C*) After an 18-h fast, WT and *Apoa5*$^{-/-}$ mice (strain FVB/NJ) were given an intravenous injection of 1.25 mg CT-APOA5 pAb or 1.25 mg nonimmune rabbit IgG (control IgG) and then refed a chow diet for 6 h. Plasma TG levels were determined at baseline (T0) and after 6 h of refeeding (T6). (*B* and *C*) Plasma TG levels in WT (*B*) and *Apoa5*$^{-/-}$ mice (*C*) at T0 and T6. A one-way ANOVA followed by Tukey's HSD post hoc test revealed that CT-APOA5 pAb significantly increased plasma TG levels in fasted WT mice (*B*) but not *Apoa5*$^{-/-}$ mice (*C*). Results show mean ± SD (n = 6 to 7/group). ***P < 0.001; ns, not significant.

ANGPTL3/8 also unfolds LPL and that the unfolding is blocked by WT-APOA5. We further suspect that the inability of APOA5Δ40 to bind to ANGPTL3/8 explains its failure to i) suppress ANGPTL3/8-mediated inhibition of LPL activity in vitro; ii) lower plasma TG levels in vivo; and iii) prevent ANGPTL3/8-mediated detachment of LPL from cultured cells.

The structure of APOA5 is unknown, but AlphaFold2 (AF2) models of C-terminal sequences in APOA5 (Q330–P366 in human APOA5; H327–G368 in mouse APOA5) predict an alpha-helical structure. Leucine and isoleucine residues in the C terminus of human APOA5 (L337, L340, L344, L347, I351, and L255), along with an invariant tryptophan (W348), are located on the same side

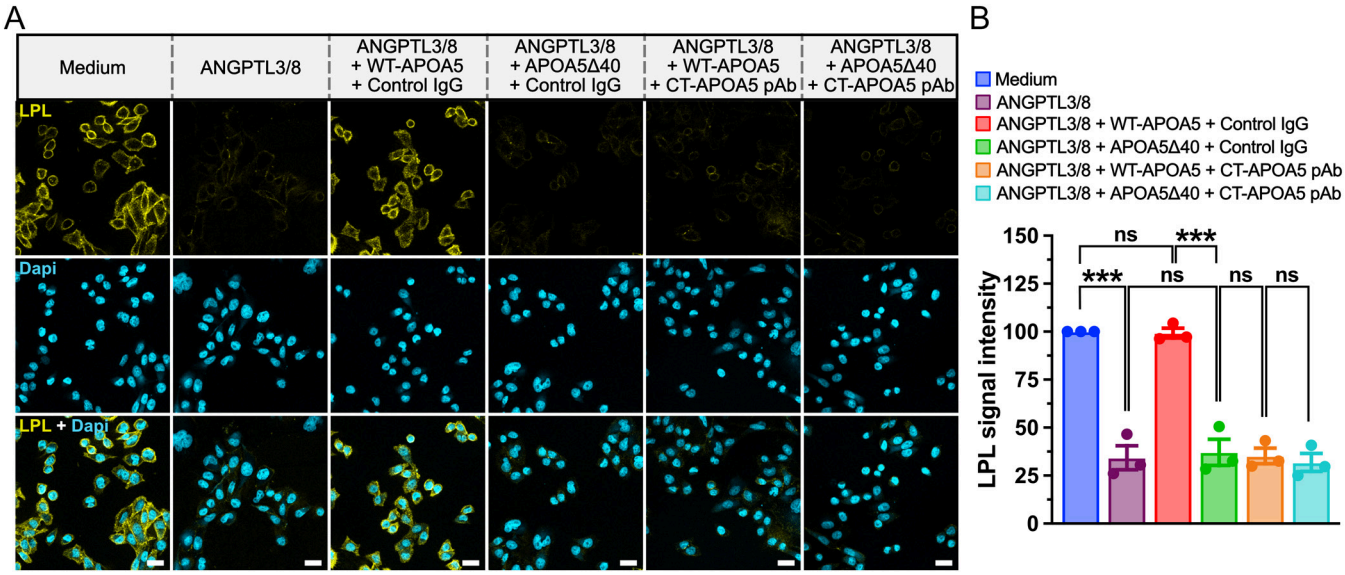

Fig. 9. An immunopurified rabbit polyclonal antibody against the C-terminal 26 residues of mouse WT-APOA5 (CT-APOA5 pAb) blocks the ability of WT mouse APOA5 to suppress ANGPTL3/8-mediated detachment of LPL from cells. CHO-K1 cells were incubated in medium in the presence or absence of 50 nM human LPL (hLPL) at 37 °C for 10 min. After washing with PBS/Ca/Mg, the cells were incubated for 15 min at 37 °C with cell culture medium alone or with medium containing 100 nM mouse ANGPTL3/8—alone or in the presence of 1.4 μM mouse WT-APOA5 or mouse APOA5Δ40 that had been preincubated with 4.2 μM CT-APOA5 pAb or control IgG. (*A*) Amounts of hLPL on the surface of cells, as judged by fluorescence microscopy, after staining cells with Alexa Fluor 555–labeled mAb 5D2. (Scale bars, 20 μm.) (*B*) LPL remaining on the surface of CHO-K1 cells, as judged by 5D2 fluorescence intensity. Each dot represents the mean ratios in each treatment group, normalized to the mean signal intensity of LPL-loaded cells incubated with medium alone (set as 100). A one-way ANOVA revealed that CT-APOA5 pAb inhibited the ability of WT-APOA5 to suppress the ability of ANGPTL3/8 to detach LPL from the surface of cells. Tukey's HSD post hoc test found no significant differences in amounts of LPL on cells that had been incubated with medium alone (in the absence of ANGPTL3/8) and cells that had been incubated with ANGPTL3/8 + mouse WT-APOA5. Amounts of LPL on cells that had been incubated with ANGPTL3/8, ANGPTL3/8 + mouse WT-APOA5 + CT-APOA5 pAb, ANGPTL3/8 + APOA5Δ40 + control IgG, or ANGPTL3/8 + APOA5Δ40 + CT-APOA5 pAb were similar and were significantly lower than in cells that had been incubated with medium alone. Similar results were observed with sensitivity analyses from a generalized linear model with logarithmic linkage and SEs clustered by experiment. Results show mean ± SEM; ***P < 0.001; ns, not significant.

of the helix, raising the possibility that they could play a role in ANGPTL3/8 binding. The parsimonious explanation for the inability of APOA5Δ40 to bind ANGPTL3/8 is that the C-terminal α-helix in APOA5 participates directly in ANGPTL3/8 binding, but another possibility would be that the truncation induces conformational changes in more distant sequences that mediate APOA5–ANGPTL3/8 interactions. A definitive understanding of the APOA5 sequences that interact with ANGPTL3/8 will require HDX-MS and structural studies.

A puzzling issue is why APOA5 evolved as an apolipoprotein carried on lipoproteins. We speculate that the presence of APOA5 on lipoproteins ensures a reservoir of APOA5 in the plasma and extends APOA5 bioavailability. Also, it is noteworthy that both lipoproteins and ANGPTL3/8 interact with LPL. Even though amounts of APOA5 on TRLs are extremely low, it is conceivable that TRL-bound pool of APOA5 could retard ANGPTL3/8-mediated unfolding of TRL-bound LPL in capillaries.

Truncating *APOA5* mutations block the ability of APOA5 to bind to ANGPTL3/8 and suppress its activity. Other pathogenic *APOA5* mutations involve different mechanisms. For example, a deletion in APOA5's signal peptide, identified in an 11-mo-old boy with severe hypertriglyceridemia, prevents secretion of APOA5 (26). Also, a p.G185C missense mutation in *APOA5* (common in East Asia) causes hypertriglyceridemia by promoting heterodisulfide bonds with other plasma proteins and limiting APOA5 association with lipoproteins (27–29). However, while pathogenic *APOA5* mutations can involve distinct molecular mechanisms, we suspect that all trigger hypertriglyceridemia by interfering with the ability of APOA5 to suppress the activity of the ANGPTL3/8 complex.

Materials and Methods

Recombinant Proteins and Antibodies. Human ANGPTL3/8, mouse ANGPTL3/8, human WT-APOA5, human LPL, an inhibitory ANGPTL3/8 monoclonal antibody (mAb IBA490, which binds to ANGPTL3/8 in a region that overlaps with the APOA5 binding site), a noninhibitory ANGPTL3/8 antibody (1G12, which binds to ANGPTL3's C-terminal fibrinogen-like domain), a mouse LPL–specific rat mAb (27A7), a human LPL–specific mouse mAb (5D2), a mouse GPIHBP1–specific rat mAb (11A12), and a hamster CD31 mAb (2H8) have been described (11, 12, 14, 30–32). Human APOA5Δ35 (resulting from a D332VfsX4 mutation), human APOA5Δ92 (from a Q275X mutation), and mouse APOA5Δ40 were produced with the techniques used to produce human WT-APOA5 (11, 12). Human APOA5Δ35 and mouse APOA5Δ40 result from the same mutation; this mutation results in the removal of 40 C-terminal amino acids in mouse APOA5 because mouse APOA5 has a 5–amino acid extension at its C terminus. APOA5 proteins contained an N-terminal albumin tag (which stabilizes APOA5). Mouse WT-APOA5 (NP_536682.2) and APOA5Δ40 contained a mouse albumin tag; human WT-APOA5, APOA5Δ35, and APOA5Δ92 contained a human albumin tag (11, 12, 30). Mouse WT-APOA5 and APOA5Δ40 (0.5 μg) were analyzed on Coomassie Blue–stained Tris-glycine/SDS 4 to 20% gradient polyacrylamide gels (SDS-PAGE) under reducing and nonreducing conditions. mAbs against a synthetic peptide corresponding to amino acids 21 to 43 (RKSLWDYFSQNSWSKGVMGQPQK) in the N terminus of mouse APOA5 (NT-APOA5 mAbs) were generated as described (11, 12, 30). A synthetic peptide corresponding to mouse APOA5 C-terminal amino acids 343 to 368 (DLWEDIAYGLQDQGHSHLSDPEGHSG) was conjugated to ovalbumin (via a cysteine added to the N terminus of the peptide) and used to create a rabbit polyclonal antibody (CT-APOA5 pAb) against mouse APOA5. The antibody was purified from 110 mL of rabbit antiserum on a Sepharose 4B–peptide immunoaffinity column. For in vivo studies involving CT-APOA5 pAb, nonimmune rabbit IgG (Jackson ImmunoResearch) that had been subjected to endotoxin removal was used as a control. A goat antiserum against APOB (Sigma AB742) was used to detect APOB in cryosections of the liver.

Size-Exclusion Chromatography and Mass Photometry. Mouse WT-APOA5 and APOA5Δ40 (100 μg) were analyzed by analytical size-exclusion chromatography (SEC) on 10/300 Superdex 200. Mouse WT-APOA5 and APOA5Δ40 were also analyzed by mass photometry (Refeyn). For each acquisition, 20 μL of each protein (10 nM in DPBS, Thermo Fisher) was pipetted into a sample well formed by Sample Well Cassettes and Ready-to-Use Sample Carrier slides (Refeyn). After loading samples, the focus was identified and secured by the autofocus function of the mass photometer, followed by interferometric scattering contrast measurement. Data were acquired for 60 s with AcquireMP, and protein mass histograms were analyzed with DiscoverMP (Refeyn). For mass calibration, the interferometric scattering contrast of 10 nM β-amylase (Sigma) was measured, and calibration curves were generated with monomeric, dimeric, and tetrameric β-amylase.

SPR Analyses. Real-time binding of mouse WT-APOA5 and mouse APOA5Δ40 to recombinant ANGPTL3/8 was assessed with a BiacoreT200 instrument. To improve performance, a double-antibody sandwich capture setup was used to obtain an oriented and homogenous presentation of the interacting proteins (33). A polyclonal rabbit anti-mouse IgG was first immobilized on a CM4 sensor chip with amine-directed chemistry. This surface was subsequently used to capture the mouse ANGPTL3/8 mAbs 1G12 (which recognizes the fibrinogen-like domain in ANGPTL3) or IBA490 (which recognizes the APOA5-binding domain of the ANGPTL3/8 complex) (100 nM of the mAbs) (12). This capture strategy provided a binding-competent ANGPTL3/8 surface (capture with 1G12) and a nonbinding ANGPTL3/8 surface (capture with inhibitory mAb IBA490). Similar levels of ANGPTL3/8 were captured by both antibodies after injecting 25 nM ANGPTL3/8 at 20 μL/min for 200 sec in running buffer [10 mM HEPES pH 7.4, 150 mM NaCl, 4 mM $CaCl_2$, 0.05% (v/v) P20, 0.2 mg/mL, and 0.05% NaN_3]. Specific interactions between APOA5 and ANGPTL3/8 were recorded with a single-cycle protocol by injecting five serial twofold dilutions of mouse WT-APOA5 or mouse APOA5Δ40 (ranging from 0.5 nM to 8 nM) at 50 μL/min at 25 °C in running buffer. Two consecutive injections of 10 mM glycine/HCl, pH 1.7 regenerated the chip, enabling a new capture cycle. After double-buffer referencing, the binding rate constants (k_{on} and k_{off}) for the APOA5–ANGPTL3/8 interaction were determined by fitting the data to a bimolecular interaction model with a mathematical model developed for single-cycle kinetics (T200 Evaluation Software 3.0; GE Healthcare).

LPL Activity Assays. The nucleotide sequence for human LPL (NP_000228.1) was inserted into pLenti6.3 vector (Invitrogen), and the lentivirus was used to create a HEK293 stable cell line. Using the nucleotide sequence for mouse LPL (NP_032535.2), we created a stable cell line for mouse LPL. Both cell lines were maintained in DMEM/F12 (3:1) (Invitrogen), 10% FBS (Hyclone), and 5 μg/mL blasticidin (Invitrogen). Cells were seeded at a density of 50,000 cells/well in 96-well plates (Costar) in growth medium (3:1 DMEM/F12, 10% FBS, 5 μg/mL blasticidin). After an overnight incubation, the cell culture medium was replaced with 80 μL of growth medium containing dilutions of human or mouse ANGPTL3/8. In some experiments, medium containing ANGPTL3/8 was preincubated for 1 h at 37 °C in the presence of 20 nM IBA490 or APOA5 proteins (human WT-APOA5, APOA5Δ35, APOA5Δ92, mouse WT-APOA5, APOA5Δ40) in the presence or absence of CT-APOA5 pAb or an equal mixture of four different NT-APOA5 mAbs). The cells were then incubated for 1 h. Next, 20 μL of 5× substrate solution, freshly prepared with 0.05% Zwittergent detergent 3-(N,N-dimethyl-octadecylammonio)-propanesulfonate (Sigma) and containing EnzChek lipase substrate BODIPY-dabcyl-labeled TG analog (Invitrogen), were added to the cells to achieve a final substrate concentration of 1 μM. Fluorescence was monitored at 1 and 30 min with a Synergy Neo2 plate reader with excitation and emission wavelengths of 485 and 516 nm, respectively. To correct for background, fluorescence readings at 1 min were subtracted from 30-min readings.

Animal Studies. CETP/APOA1 transgenic mice and *Apoa5*$^{-/-}$ mice (FVB/NJ strain) have been described previously (12, 14). C57BL/6 mice from The Jackson Laboratory were used as controls for studies with CETP/APOA1 transgenic mice. WT mice (FVB/NJ strain) from Charles River Laboratories were used as controls for studies with *Apoa5*$^{-/-}$ mice (FVB/NJ strain). Mice were maintained in a barrier facility with a 12-h light–dark cycle and fed a chow diet ad libitum unless otherwise stated. Studies with C57BL/6 mice and CETP/APOA1 transgenic mice were approved by the Institutional Animal Care and Use Committee of Eli Lilly & Co; studies with *Apoa5*$^{-/-}$ mice were approved by UCLA's Animal Research Committee.

TG Measurements. Serum TG levels were determined in C57BL/6 and CETP/APOA1 transgenic mice with a Roche Cobas instrument. Plasma TG levels in *Apoa5*$^{-/-}$ mice and wild-type controls were determined with a TG Colorimetric Assay Kit (Cayman).

To examine the effects of fasting and feeding on TG levels, serum was collected from 16- to 20-wk-old C57BL/6 mice ($n = 10$ mice/group) after an overnight fast and 4 h after refeeding a chow diet.

The effects of mouse WT-APOA5, mouse APOA5Δ40, and mAb IBA490 on TG levels were assessed in CETP/APOA1 transgenic mice and *Apoa5*$^{-/-}$ mice. In male 16- to 20-wk-old CETP/APOA1 transgenic mice, serum TG levels were measured before and 1 h, 3 h, and 6 h after a subcutaneous injection of vehicle alone (PBS), IBA490 (2.5 nmole/mouse), mouse WT-APOA5 (1.0 nmole/mouse), or APOA5Δ40 (1.0 nmole/mouse) ($n = 7$/group). Plasma TG levels in 10- to 16-wk-old male *Apoa5*$^{-/-}$ mice were measured before and 4 h after an intravenous injection of vehicle (PBS), mouse WT-APOA5 (0.5 nmole), or mouse APOA5Δ40 (0.5 nmole) ($n = 6$ to 7/group). As a control, *Apoa5*$^{-/-}$ mice ($n = 2$/group) were given an intravenous injection of mAb IBA490 (1.25 nmole/mouse).

To assess the functional relevance of C-terminal sequences in mouse APOA5, 10- to 16-wk-old WT and *Apoa5*$^{-/-}$ mice (FVB/NJ strain) were fasted for 18 h and then given an intravenous injection of 1.25 mg of CT-APOA5 pAb or nonimmune rabbit IgG. After the injection, the mice were allowed to refeed a chow diet. Plasma TG levels were obtained at baseline (before antibody injection) and 6 h after refeeding.

Mouse ANGPTL3/8 Immunoassay. MesoScale Discovery (MSD) streptavidin plates were washed with TBST (Tris buffered saline containing 10 mmol/L Tris, pH 7.40, 150 mmol/L NaCl, and 1 mL/L Tween 20) and blocked with TBS containing 1% bovine serum albumin (BSA) for 1 h. After washing, wells were incubated with a biotinylated mouse ANGPTL3–specific capture mAb for 1 h. After washing, 50 μL of serial dilutions of recombinant mouse ANGPTL3/8 (for a standard curve) were added to wells in assay buffer (50 mM HEPES, pH 7.40, 150 mM NaCl, 1% Triton X-100, 5 mM EDTA, and 5 mM EGTA). Mouse serum samples were diluted 1:10 in assay buffer, added to the wells, and incubated for 2 h. After washing, 50 μL of a ruthenium-labeled mouse ANGPTL3/8-specific mAb were added to the wells for 1 h. After washing, 150 μL of MSD "read buffer" was added, and ruthenium electrochemiluminescence was detected with an MSD plate reader.

Mouse APOA5 Immunoassay. MSD streptavidin plates were washed with TBST and blocked with TBS containing 1% BSA for 1 h. After washing, wells were incubated with a biotinylated NT-APOA5 mAb for 1 h. After washing, 50 μL of recombinant mouse APOA5 (serially diluted for a standard curve) or mouse serum samples (diluted 1:100 in assay buffer) were added to wells and incubated for 2 h. After washing, 50 μL of a ruthenium-labeled CT-APOA5 pAb was added and incubated for 1 h. After washing, 150 μL of MSD read buffer was added, and ruthenium electrochemiluminescence was detected with an MSD plate reader.

Assessing Amounts of LPL in Blood Vessels. Intracapillary levels of mouse LPL, GPIHBP1, and CD31 were examined as described (14). Briefly, 4 h after giving *Apoa5*$^{-/-}$ mice an intravenous injection of PBS, WT-APOA5 (0.5 nmole/mouse), or APOA5Δ40 (0.5 nmole/mouse) (and 6 h after giving wild-type mice an intravenous injection of 1.25 mg of the CT-APOA5 pAb or nonimmune rabbit IgG), the mice were given an intravenous injection of Alex Fluor–labeled 27A7, 11A12, and 2H8 (120 μg of each mAb). Ten minutes later, the mice were killed; the vasculature was perfused and fixed; and heart and BAT sections were prepared for fluorescence microscopy. Images were recorded with an LSM980 microscope (Zeiss) with a 20× objective. We also performed studies in which mouse WT-APOA5– or APOA5Δ40-treated *Apoa5*$^{-/-}$ mice (0.5 nmole/mouse) were given an intravenous injection of IRDye800-11A12 and IRDye680-27A7. Sections of the heart and BAT were prepared, and infrared signals were quantified with a LICOR infrared scanner.

ANGPTL3/8-Mediated Release of LPL from the Surface of Cells. Amounts of LPL on the surface of cultured cells were measured as described (14). Briefly, CHO-K1 cells (ATCC CCL-61) were loaded with 50 nM human LPL in serum-free medium at 37 °C. After 10 min, cells were washed with PBS/Ca/Mg and incubated at 37 °C for 15 min with serum-free medium alone or medium containing 0.1 U/mL heparin, 100 nM ANGPTL3/8, 100 nM ANGPTL3/8 with 1.4 μM mouse WT-APOA5 or APOA5Δ40, 100 nM ANGPTL3/8 with 1.4 μM mouse WT-APOA5 in the presence of 4.2 μM CT-APOA5 pAb or control IgG, or 100 nM ANGPTL3/8 with 1.4 μM APOA5Δ40 in the presence of 4.2 μM CT-APOA5 pAb or control IgG. The cells were washed three times in PBS/Ca/Mg and blocked in 10% donkey serum in PBS/Ca/Mg at 4 °C for 1 h. To quantify the amounts of human LPL on the surface of cells, nonpermeabilized cells were stained with Alexa Fluor 555–labeled 5D2 (3 μg/mL) in 3% donkey serum/PBS/Ca/Mg at 4 °C for 1 h (14, 31). After washing the cells three times in 3% donkey serum/PBS/Ca/Mg and twice with PBS/Ca/Mg, the cells were fixed, stained with DAPI, rinsed, and mounted. Images were recorded with an LSM980 microscope (Zeiss) with a 20× objective.

Statistical Analyses and Data Availability. Data show mean ± SD or mean ± SEM. A four-parameter logistic nonlinear regression model was used to fit LPL activity curves. For mouse ANGPTL3/8 and APOA5 immunoassays, MSD software was used for curve fitting (5-parameter fit with $1/y^2$ weighting). Between-group differences in serum TG levels were assessed with one-way ANOVA and post hoc pairwise comparisons using Tukey's honestly significant difference (HSD) post hoc test was used for multiple group comparisons. We established the robustness of these statistical tests with supplementary sensitivity analyses involving generalized linear regression models with logarithmic linkage and clustered robust SEs for within-experiment correlation. Statistical analyses were conducted using JMP 13 (SAS Cary, NC), Prism 9.0 (GraphPad), and Stata SE 18.1 (StataCorp) software. For all studies, a two-sided P value <0.05 was considered statistically significant.

Data, Materials, and Software Availability. All study data are included in the article and/or supporting information.

ACKNOWLEDGMENTS. This study was funded by Eli Lilly & Co., grants from the National Heart, Lung, and Blood Institute (HL146358, HL087228, and HL139725), and grants from the Leducq Foundation (12CVD04 and 23CVD02). We thank Sydney Law, Julian Davies, Oliver Schroeder, and Melissa Bellinger for assistance.

Author affiliations: [a]Lilly Research Laboratories, Eli Lilly and Company, Indianapolis, IN 462585; [b]Department of Medicine, David Geffen School of Medicine, University of California, Los Angeles, CA 90095; [c]Department of Human Genetics, David Geffen School of Medicine, University of California, Los Angeles, CA 90095; [d]Finsen Laboratory, Centre for Cancer and Organ Diseases, Copenhagen University Hospital-Rigshospitalet, DK-2200 Copenhagen N, Denmark; [e]Finsen Laboratory, Biotech Research and Innovation Centre, University of Copenhagen, DK-2200 Copenhagen N, Denmark; and [f]Division of Experimental Medicine, Beth Israel Deaconess Medical Center, Boston, MA 02215

Author contributions: M.P., S.G.Y., and R.J.K. designed research; Y.Q.C., Y.Y., E.Y.Z., T.P.B., H.L., Y.W., M.E., K.X., H.J., J.L.S., A.K., A.M.R., D.B., Z.L., R.W.S., and Y.Q. performed experiments; A.K., G.B., M.P., and R.J.K. contributed new reagents/analytic tools; Y.Q.C., Y.Y., N.J., M.P., S.G.Y., and R.J.K. analyzed data; and Y.Y., S.G.Y., and R.J.K. wrote the paper.

1. L. A. Pennacchio *et al.*, An apolipoprotein influencing triglycerides in humans and mice revealed by comparative sequencing. *Science* **294**, 169–173 (2001).
2. X. Prieur, H. Coste, J. C. Rodriguez, The human apolipoprotein AV gene is regulated by peroxisome proliferator-activated receptor-alpha and contains a novel farnesoid X-activated receptor response element. *J. Biol. Chem.* **278**, 25468–25480 (2003).
3. N. Vu-Dac *et al.*, Apolipoprotein A5, a crucial determinant of plasma triglyceride levels, is highly responsive to peroxisome proliferator-activated receptor alpha activators. *J. Biol. Chem.* **278**, 17982–17985 (2003).
4. A. E. Schultze, W. E. Alborn, R. K. Newton, R. J. Konrad, Administration of a PPAR-alpha agonist increases serum apolipoprotein AV levels and the apolipoprotein AV/apolipoprotein CIII ratio. *J. Lipid Res.* **46**, 1591–1595 (2005).
5. H. N. van der Vliet *et al.*, Apolipoprotein AV: A novel apolipoprotein associated with an early phase of liver regeneration. *J. Biol. Chem.* **276**, 44512–44520 (2001).
6. P. J. O'Brien *et al.*, The novel apolipoprotein A5 is present in human serum, is associated with VLDL, HDL, and chylomicrons, and circulates at very low concentrations compared with other apolipoproteins. *Clin. Chem.* **51**, 351–359 (2005).
7. W. E. Alborn, M. G. Johnson, M. J. Prince, R. J. Konrad, Definitive N-terminal protein sequence and further characterization of the novel apolipoprotein A5 in human serum. *Clin. Chem.* **52**, 514–517 (2006).
8. R. B. Weinberg *et al.*, Structure and interfacial properties of human apolipoprotein AV. *J. Biol. Chem.* **278**, 34438–34444 (2003).
9. J. A. Beckstead *et al.*, The C terminus of apolipoprotein AV modulates lipid-binding activity. *J. Biol. Chem.* **282**, 15484–15489 (2007).
10. A. Lookene, J. A. Beckstead, S. Nilsson, G. Olivecrona, R. O. Ryan, Apolipoprotein AV–heparin interactions: Implications for plasma lipoprotein metabolism. *J. Biol. Chem.* **280**, 25383–25387 (2005).
11. Y. Q. Chen *et al.*, ApoA5 lowers triglyceride levels via suppression of ANGPTL3/8–mediated LPL inhibition. *J. Lipid. Res.* **62**, 100068 (2021).

12. D. Balasubramaniam *et al.*, An anti-ANGPTL3/8 antibody decreases circulating triglycerides by binding to a LPL-inhibitory leucine zipper-like motif. *J. Lipid. Res.* **63**, 100198 (2022).
13. D. Gaudet *et al.*, A first-in-human single ascending dose study of a monoclonal antibody against the ANGPTL3/8 complex in subjects with mixed hyperlipidemia. *Atherosclerosis* **355**, 12 (2022).
14. Y. Yang *et al.*, Hypertriglyceridemia in *Apoa5*$^{-/-}$ mice results from reduced amounts of lipoprotein lipase in the capillary lumen. *J. Clin. Invest.* **133**, e172600 (2023).
15. E. Mendoza-Barberá *et al.*, Structural and functional analysis of APOA5 mutations identified in patients with severe hypertriglyceridemia. *J. Lipid Res.* **54**, 649–661 (2013).
16. A. J. Hooper, J. Kurtkoti, I. Hamilton-Craig, J. R. Burnett, Clinical features and genetic analysis of three patients with severe hypertriglyceridaemia. *Ann. Clin. Biochem.* **51**, 485–489 (2014).
17. A. Schutz Geschwender, Y. Zhang, T. Holt, D. McDermitt, D. Olive, Quantitative, two-color western blot detection with infrared fluorescence. *LI-COR Biosci.* **2**, 1–7 (2004).
18. W. Song *et al.*, The lipoprotein lipase that is shuttled into capillaries by GPIHBP1 enters the glycocalyx where it mediates lipoprotein processing. *Proc. Natl. Acad. Sci. U.S.A.* **120**, e2313825120 (2023).
19. S. Kersten, Long-lost friend is back in the game. *J. Lipid Res.* **62**, 100072 (2021).
20. K. K. Kristensen *et al.*, Unfolding of monomeric lipoprotein lipase by ANGPTL4: Insight into the regulation of plasma triglyceride metabolism. *Proc. Natl. Acad. Sci. U.S.A.* **117**, 4337–4346 (2020).
21. K. Z. Leth-Espensen *et al.*, The intrinsic instability of the hydrolase domain of lipoprotein lipase facilitates its inactivation by ANGPTL4-catalyzed unfolding. *Proc. Natl. Acad. Sci. U.S.A.* **118**, e2026650118 (2021).
22. A. Kumari *et al.*, Inverse effects of APOC2 and ANGPTL4 on the conformational dynamics of lid-anchoring structures in lipoprotein lipase. *Proc. Natl. Acad. Sci. U.S.A.* **120**, e2221888120 (2023).
23. W. Dijk *et al.*, Angiopoietin-like 4 promotes intracellular degradation of lipoprotein lipase in adipocytes. *J. Lipid Res.* **57**, 1670–1683 (2016).
24. W. Dijk *et al.*, Regulation of angiopoietin-like 4 and lipoprotein lipase in human adipose tissue. *J. Clin. Lipidol.* **12**, 773–783 (2018).
25. S. Kersten, Role and mechanism of the action of angiopoietin-like protein ANGPTL4 in plasma lipid metabolism. *J. Lipid Res.* **62**, 100150 (2021).
26. K. Albers *et al.*, Homozygosity for a partial deletion of apolipoprotein AV signal peptide results in intracellular missorting of the protein and chylomicronemia in a breast-fed infant. *Atherosclerosis* **233**, 97–103 (2014).
27. C. R. Pullinger *et al.*, An apolipoprotein AV gene SNP is associated with marked hypertriglyceridemia among Asian-American patients. *J. Lipid Res.* **49**, 1846–1854 (2008).
28. V. Sharma *et al.*, Aberrant hetero-disulfide bond formation by the hypertriglyceridemia-associated p.Gly185Cys APOA5 variant (rs2075291). *Arterioscler. Thromb. Vasc. Biol.* **34**, 2254–2260 (2014).
29. Y. Han *et al.*, Genome-wide association study identifies a missense variant at APOA5 for coronary artery disease in multi-ethnic cohorts from southeast Asia. *Sci. Rep.* **7**, 17921 (2017).
30. Y. Q. Chen *et al.*, Angiopoietin-like protein 8 differentially regulates ANGPTL3 and ANGPTL4 during postprandial partitioning of fatty acids. *J. Lipid Res.* **61**, 1203–1220 (2020).
31. J. G. Luz *et al.*, The structural basis for monoclonal antibody 5D2 binding to the tryptophan-rich loop of lipoprotein lipase. *J. Lipid Res.* **61**, 1347–1359 (2020).
32. S. A. Bogen, H. S. Baldwin, S. C. Watkins, S. M. Albelda, A. K. Abbas, Association of murine CD31 with transmigrating lymphocytes following antigenic stimulation. *Am. J. Pathol.* **141**, 843–854 (1992).
33. J. M. Leth, H. D. T. Mertens, K. Z. Leth-Espensen, T. J. D. Jørgensen, M. Ploug, Did evolution create a flexible ligand-binding cavity in the urokinase receptor through deletion of a plesiotypic disulfide bond? *J. Biol. Chem.* **294**, 7403–7418 (2019).